JOURNAL OF GEOPHYSICAL RESEARCH, VOL. 115, D02305, doi:10.1029/2009JD012536, 2010

Characteristics of atmospheric transport into the Antarctic troposphere

A. Stohl[1] and H. Sodemann[1]

Received 25 May 2009; revised 8 September 2009; accepted 15 September 2009; published 23 January 2010.

[1] We have developed a 5.5 year climatology of atmospheric transport into the Antarctic troposphere, which uses the same data set and methods as described in a recent study for the Arctic. This allows direct comparisons of transport properties for the two polar regions. The climatology is based on a simulation with the Lagrangian particle dispersion model FLEXPART, where the model atmosphere was globally filled with particles. Transport characteristics as well as emission sensitivities were derived from 6 hourly particle positions. We found that the probability for near-surface air to originate from the stratosphere on a time scale of 10 days is an order of magnitude higher near the South Pole than near the North Pole, a result of higher topography and descent that partly compensates for the flow of air down the Antarctic Plateau with the katabatic winds. The stratospheric influence is largest in fall, which is opposite to the seasonality in the Arctic. Stratospheric influence is much smaller over the shelf ice regions and in a band around Antarctica. The average time for which air near the surface has been exposed to continuous darkness in July (continuous light in January) is longest over the Ronne Ice Shelf and Ross Ice Shelf at ~11 days (20 days). We calculated how sensitive Antarctic air masses are to emission input up to 30 days before arriving in Antarctica if removal processes are ignored. The emission sensitivity shows strong meridional gradients and, as a result, is generally low over South America, Africa, and Australia. For a 10 day time scale, the largest emission sensitivities over these continents are 1–2 orders of magnitude smaller than over Eurasia for transport to the Arctic, showing that foreign continents have a much smaller potential to pollute the Antarctic than the Arctic troposphere. Emission sensitivities and derived black carbon (BC) source contributions over South America, Africa, and Australia are substantially (a factor 10 for Africa) larger in winter than in summer. In winter, biomass burning contributes more BC than anthropogenic sources. For typical aerosol lifetimes of 5–10 days, ship emissions south of 60°S account for half of the total BC concentrations in the lowest 1000 m of the atmosphere south of 70°S in December. The increasing number of tourists visiting Antarctica and fishing vessels operating close to Antarctica are, therefore, a matter of concern.

Citation: Stohl, A., and H. Sodemann (2010), Characteristics of atmospheric transport into the Antarctic troposphere, *J. Geophys. Res.*, *115*, D02305, doi:10.1029/2009JD012536.

1. Introduction

[2] Even though Antarctica is the most remote of all continents, the local pollutant emissions due to the increasing human presence [*Shirsat and Graf*, 2009] and pollution imported from other continents are matters of concern. Aerosols and short-lived trace gases can affect the fragile Antarctic ecosystem and potentially also have climate effects. *Quinn et al.* [2008] have summarized a number of processes by which aerosols and short-lived trace gases can cause a warming of the Arctic. While concentration levels are much lower, the same processes operate also in the Antarctic. Ice cores from Antarctica, which in addition to climate proxies also record past aerosol concentration levels [*Wolff and Peel*, 1985; *McConnell et al.*, 2007], may allow studying the interplay between atmospheric composition and climate. An important requirement for their interpretation, however, is a good understanding of atmospheric transport into and within the Antarctic troposphere.

[3] Atmospheric transport is determined by the unique circulation patterns over Antarctica. Except for austral summer, the small incoming shortwave radiation flux, the high albedo, and the weak greenhouse gas effect (a consequence of dryness and great altitude) cause strong net radiative cooling at the surface and the formation of an extreme temperature inversion in the lowest few hundred meters of the atmosphere [*Connolley*, 1996; *van den Broeke and van Lipzig*, 2003]. Underneath the inversion top, cold air persistently drains down the gently sloping surfaces (at

[1]Department of Regional and Global Pollution Issues, Norwegian Institute for Air Research, Kjeller, Norway.

0148-0227/10/2009JD012536$09.00

an angle, due to the balance between the pressure force, the Coriolis force and the drag force) in the Antarctic interior [*Parish and Bromwich*, 2007]. It eventually falls down the steep slopes and valleys of the coastal regions at speeds that are among the highest observed surface wind velocities on Earth (see *van den Broeke and van Lipzig* [2003] and *Parish and Bromwich* [2007] for analyses of the near-surface wind field over Antarctica). The mass flux associated with these katabatic winds is significant even at the global scale [*Dalu et al.*, 1993]. The mass lost in the outflow must be replaced by subsidence over Antarctica [*Van de Berg et al.*, 2007] which in turn is fed in the middle and upper troposphere by convergence of air into a cyclonic vortex above Antarctica [*James*, 1989]. Some of the air descending into the Antarctic boundary layer may originate in the stratosphere [*Roscoe*, 2004] where intense cooling maintains a strong and stable vortex in winter.

[4] Over the seas surrounding Antarctica, there is net upward transport [*Parish and Bromwich*, 2007; *Van de Berg et al.*, 2007] accomplished partly by the globally highest frequency of cyclones [*Simmonds et al.*, 2003; *Wernli and Schwierz*, 2006]. The cyclones can interrupt the katabatic outflow from the continent and are responsible for much of the moisture transport toward the ice sheet [*Van Lipzig and van den Broeke*, 2002]. The strong cyclonic winds also mobilize large amounts of sea salt, an important aerosol over Antarctica [*Fischer et al.*, 2007], and marine biological sources dominate the non-sea-salt aerosol sulphate over Antarctica [*Minikin et al.*, 1998; *Savoie et al.*, 1992]. The cyclones often also bring enhancements in radon-222 [*Wyputta*, 1997] or black carbon (BC) aerosols [*Murphey and Hogan*, 1992] that must originate on other continents. In connection with blocking highs, relatively warm moist aerosol rich air can intrude with cyclones even over the Antarctic Plateau [*Massom et al.*, 2004] and to the South Pole [*Hogan et al.*, 1982; *Arimoto et al.*, 2008].

[5] While the strong influence of marine sources on Antarctic aerosol concentrations is obvious, the transport of material from other continents is not often directly observed. A few individual events have been documented, such as the transport of dust from Patagonia [*Gasso and Stein*, 2007] or smoke from biomass burning in South America [*Evangelista et al.*, 2007; *Pereira et al.*, 2006] to the tip of the Antarctic peninsula. *Fiebig et al.* [2009] discovered transport of biomass burning aerosol from South America to an inland site on Queen Maude Land. *Wyputta* [1997] tentatively linked an increase in radon-222 concentrations at the coastal Georg von Neumayer station to transport from South America. Another method of attributing deposited material to its sources is geochemical fingerprinting of Antarctic ice core dust. Using this technique, South America was identified as the dominant dust source region during glacial periods [*Delmonte et al.*, 2004] but a substantial contribution of dust from Australia was revealed during interglacial periods [*Revel-Rolland et al.*, 2006].

[6] Owing to the remoteness of Antarctica and difficulties with identifying clear transport events in the atmospheric measurement data, models have often been used to attribute pollution in Antarctica to its sources. For example, *Krinner and Genthon* [2003] initialized tracers with fixed lifetimes over the Southern Hemisphere continents in an atmospheric general circulation model.

[7] They found that transport to Antarctica from South America is fastest, followed by transport from Australia, while transport from South Africa is much slower. This is in agreement with a recent study by *Li et al.* [2008] who simulated the transport of dust from the different source continents. They also found a relatively strong influence of dust from the Northern Hemisphere in the upper troposphere over Antarctica, a finding which cannot be verified because of a lack of measurement data. However, *Yurganov* [1997] showed that in Antarctica measured carbon monoxide concentrations averaged over the entire tropospheric column are greater than the concentrations near the surface, indicating a stronger influence from continental sources and maybe the Northern Hemisphere aloft. Generally, transport models have not often been compared directly to observation data from Antarctica, probably because of a lack of model skill. In one comparison, the modeled BC at Halley station and at the South Pole had almost the opposite seasonal cycle as the observations [*Wolff and Cachier*, 1998].

[8] Statistical studies of transport to Antarctica have also been performed using trajectory calculations for single measurement stations or ice core drilling sites. An example is the study of *Kottmeier and Fay* [1998] who presented 3 year statistics of 5 day back trajectories from the Neumayer station. Trajectories have also been used to identify where the moisture for precipitation events is coming from [e.g., *Reijmer et al.*, 2002; *Helsen et al.*, 2006; *Suzuki et al.*, 2008] and for water isotope modeling [*Schlosser et al.*, 2008].

[9] This paper presents a transport climatology for the Antarctic troposphere, which is built on the same data set and the same methods as used by *Stohl* [2006] for a transport climatology for the Arctic. This allows direct comparisons of transport characteristics for the two regions. The climatology is not specific to a single location and will present time scales of transport within Antarctica and from various regions outside, with a focus on conditions near the surface. In a related paper, *Sodemann and Stohl* [2009] use the same data set and a moisture source diagnostic to identify where the precipitation falling over Antarctica has its evaporation sources. For the reader's convenience, Figure 1 shows maps of sea ice concentration around Antarctica in September and February, as well as Antarctic topography and annual snow accumulation, and marks geographical features referred to in this paper.

2. Model Calculations

[10] The data set of *Stohl* [2006] which is used here was generated with the Lagrangian particle dispersion model FLEXPART [*Stohl et al.*, 1998, 2005; *Stohl and Thomson*, 1999] (see also http://transport.nilu.no/flexpart) for a 5.5 year period (27 October 1999 until 1 May 2005). FLEXPART was driven with operational analyses from the European Centre for Medium-Range Weather Forecasts [*White*, 2002] with $1^\circ \times 1^\circ$ resolution (derived from T319 spectral truncation) and 60 model levels (14 below 1500 m above ground level (a.g.l.)). Analyses at 0000, 0600, 1200, and 1800 UTC and 3 hour forecasts at 0300, 0900, 1500, and 2100 UTC were used.

[11] FLEXPART calculates trajectories using the mean winds interpolated from the ECMWF analyses plus random

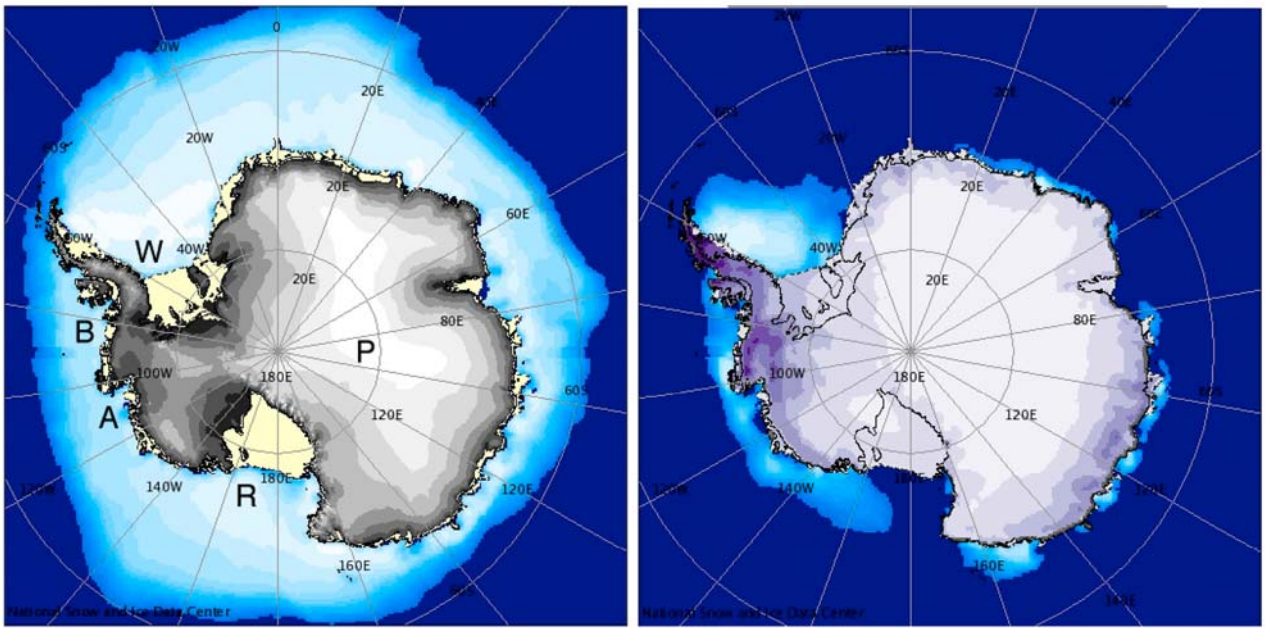

Figure 1. (left) Maps of the Antarctic topography (gray shading) and sea ice concentration (blue-white shading) in September and (right) annual snow accumulation (violet shading) and sea ice concentration (blue-white shading) in February. Sea ice concentrations are averages over the period 1979–2007, with contour shadings ranging from 15% (light blue) to 100% (white). In Figure 1 (left), geographic features mentioned in the text are denoted by letters: Amundsen (A), Bellingshausen (B), Weddell (W), and Ross (R) seas; and Antarctic Plateau (P). Maps were generated using an Internet Web page of the National Snow and Ice Data Center (http://www.nsidc.org/index.html).

motions that account for turbulence. In the boundary layer, Langevin equations for Gaussian turbulence [*Stohl and Thomson*, 1999] are solved. For moist convective transport, FLEXPART uses the scheme of *Emanuel and Živković-Rothman* [1999], as described and tested by *Forster et al.* [2007]. In order to maintain high accuracy around the pole, FLEXPART advects particles on a polar stereographic projection poleward of 75°.

[12] At the start of the model simulation, the global atmosphere was "filled" homogeneously with 1.4 million particles. Particles were then allowed to move freely, and their positions and meteorological data interpolated from the ECMWF analyses were recorded in output files every 6 hours. As particles were not repositioned during the simulation, the model must not violate the so-called well-mixed criterion [*Thomson*, 1987], i.e., accumulate particles or leave voids in particular regions. This was largely the case [*Stohl*, 2006]. All analyses were done on a 3° longitude × 2° latitude grid with 9 layers and are presented as monthly or seasonal (summer: December, January, February; fall: March, April, May; winter: June, July, August; spring: September, October, November) mean values.

[13] While the ECMWF data used can resolve synoptic-scale flow patterns, the strong temperature inversions often found over Antarctica and the katabatic winds especially near the coast are certainly not fully resolved and would require higher resolution. Another problem may be that the turbulence parameterizations have not been developed specifically for the extreme Antarctic conditions but have been derived from field experiments in the middle latitudes. We concentrate our analyses on the lowest 100–1000 m of the atmosphere, which is probably not fully representative of near-surface air given the substantial structure that may exist even below 100 m in the Antarctic atmosphere. This is a compromise taking into account the current limitations of the ECMWF data and other global meteorological analyses.

3. Results

3.1. Transport From the Stratosphere

[14] To determine the impact of stratospheric air in the Antarctic troposphere, we counted the time since particles crossed the thermal tropopause [*World Meteorological Organization*, 1986] for the last time. The thermal tropopause is not well defined over Antarctica in winter [*Court*, 1942; *Neff*, 1999; *Zängl and Hoinka*, 2001] but was used here for consistency with the Arctic study of *Stohl* [2006]. In order to avoid false positive tropopause diagnoses because of the strong temperature gradients due to cooling at the surface, our algorithm starts searching for the thermal tropopause from 2.5 km above ground level. Over the Antarctic Plateau, the tropopause may occasionally be lower than this minimum value, which could lead to a slight underestimation of the stratospheric influence in our study. As in *Stohl* [2006], we show maps of the probability that air residing in the lowest 500 m of the atmosphere has come from the stratosphere within 10 days. Using shorter time scales results in very small fractions of stratospheric air, whereas using longer time scales yields similar but smoother spatial patterns.

[15] Throughout the year, the probabilities for transport from the stratosphere are lowest in a subpolar band around

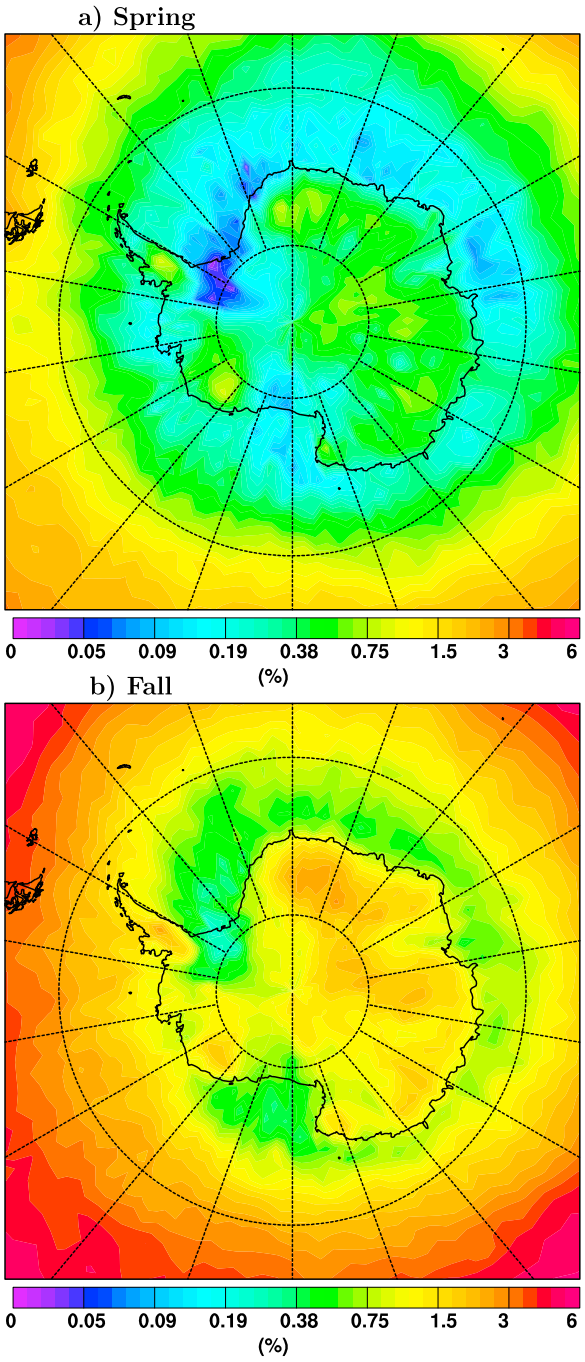

Figure 2. Probability that air in the lowest 500 m has come from the stratosphere within the last 10 days for (a) spring (September, October, and November) and (b) fall (March, April, and May).

Antarctica, especially over the Ronne and Ross ice shelf regions (Figure 2). There, the transport probabilities are 2 orders of magnitude lower than in the middle and subtropical latitudes where they can reach 10%. This strong meridional gradient in stratospheric influence is similar to what was found for the Arctic [*Stohl*, 2006, Figure 6] where, however, transport probabilities decrease further toward the North Pole. In contrast, transport probabilities over the Antarctic interior are some factor of 4 higher than those over the subpolar band. This is in agreement with a maximum of stratospheric influence near the South Pole found by *James et al.* [2003, Figure 1]. The transport probabilities of the order of 1% over the Antarctic Plateau are almost an order of magnitude (depending on season) higher than in the most isolated parts of the high Arctic but are comparable to those over Greenland [see *Stohl*, 2006, Figure 6] which is located away from the pole. This confirms the picture of *Roscoe* [2004], where air is brought down in the stratosphere by the Brewer-Dobson circulation and transported down further into the troposphere to replace the air flowing down the Antarctic Plateau with the katabatic winds [*James*, 1989]. The relatively strong stratospheric influence over Antarctica has important implications for ozone [*Helmig et al.*, 2007] as well as for reactive nitrogen [*Davis et al.*, 2008], for which the stratosphere is a source.

[16] The patterns of stratospheric influence in Figure 2 can be well understood by the two mechanisms bringing down stratospheric air: stratospheric intrusions occurring in midlatitude cyclones [*James et al.*, 2003] and general subsidence over Antarctica [*Roscoe*, 2004]. Stratospheric influence is minimal in the zonal band between the latitudes where these two mechanisms operate. Even though cyclones are frequent in this region [*Simmonds et al.*, 2003], these cyclones, unlike those further north or in the Northern Hemisphere, are shallow and do not extend into the tropopause region [*Carrasco and Bromwich*, 1994; *Eckhardt et al.*, 2004]. The subpolar band of low stratospheric influence can also be understood in terms of the distribution of potential temperature Θ. Figure 3 shows a vertical section of Θ, with the section's left half running along 29.5°E from 60°S to the pole and its right half running from the pole along 169.5°W. The lowest Θ values occur near the surface over the shelf ice regions (near 80°S, 169.5°W in Figure 3). As the cold air from the Antarctic interior flows down to the coast with the katabatic winds and warms adiabatically, radiative cooling continues and Θ decreases, thus producing the most isolated air. As we shall see in following sections, this air is the most "aged" also in terms of time scales other than that for transport from the stratosphere.

[17] Figure 4 shows time series of the transport probabilities of originally stratospheric air masses for a box (70°S–86°S, 0°E–141°E) located over the Antarctic Plateau. At 3–5 km agl, there is a strong and systematic seasonal cycle, with maximum transport probabilities of 60–80% in late summer and fall, and minimum transport probabilities of 10% in late winter. This seasonality is contrary to that in the Arctic [*Stohl*, 2006] but it is in agreement with the opposite seasonal cycles of tropopause altitudes in the Arctic and Antarctic [*Zängl and Hoinka*, 2001], which is a result of the cold and stable stratospheric vortex over Antarctica in winter. A less clear but similar seasonal cycle of stratospheric influence is also found near the surface. Notice also the strong vertical gradient of the stratospheric influence, with transport probabilities for the layer 0.5–1.5 km agl higher by more than a factor of 2 than transport probabilities below 0.1 km agl, reflecting the extremely stable layering of the lowermost troposphere over the Antarctic Plateau (see Figure 3) and the strong cooling required to bring air down to the surface. In reality the stability is probably even higher than in the ECMWF data. Furthermore, strong inversions can be found below 100 m such that the air near the surface

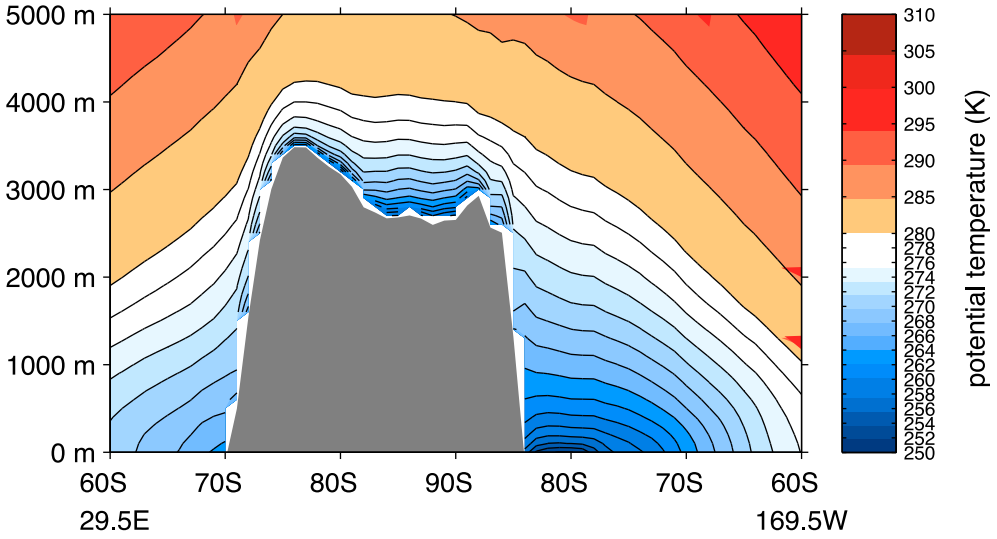

Figure 3. Vertical section of the potential temperature, averaged over the years 2003 and 2004, from 60°S along 29.5°E to the South Pole and from the South Pole along 169.5°W to 60°S.

will tend to be even more isolated than our results for the lowest 100 m indicate.

[18] The seasonality of stratospheric influence is confirmed by atmospheric measurements of the radionuclide beryllium-7, which is mostly produced in the stratosphere and upper troposphere, attaches to aerosols and is removed from the atmosphere by deposition together with the aerosols. We have used monthly data from the Environmental Measurements Laboratory's Surface Air Sampling Project (SASP) (downloaded from http://www.eml.st.dhs.gov/databases/SASP/on 7 September 2009) from four Antarctic stations to calculate the mean annual variation of beryllium-7. At both South Pole station and Mawson station (68°S, 63°E), beryllium-7 activity concentrations are about twice as high in summer (late summer at Mawson) than in winter, in agreement with the report of *Savoie et al.* [1992] and in agreement with our seasonal cycle of stratospheric influence. Concentrations at two coastal sites on the Antarctic Peninsula (Palmer station) and on King George Island (Marsh station) show rather flat seasonal cycles and much lower concentrations, most likely due to more efficient deposition of beryllium-7. Another radioactive isotope produced by natural processes in the stratosphere and also injected into the stratosphere by nuclear bomb tests is radioactive tritium. Tritium levels recorded in ice cores on the Antarctic Plateau are surprisingly high [*Fourré et al.*, 2006]. While these high concentrations are mainly explained by the low accumulation rates in the Antarctic interior and show

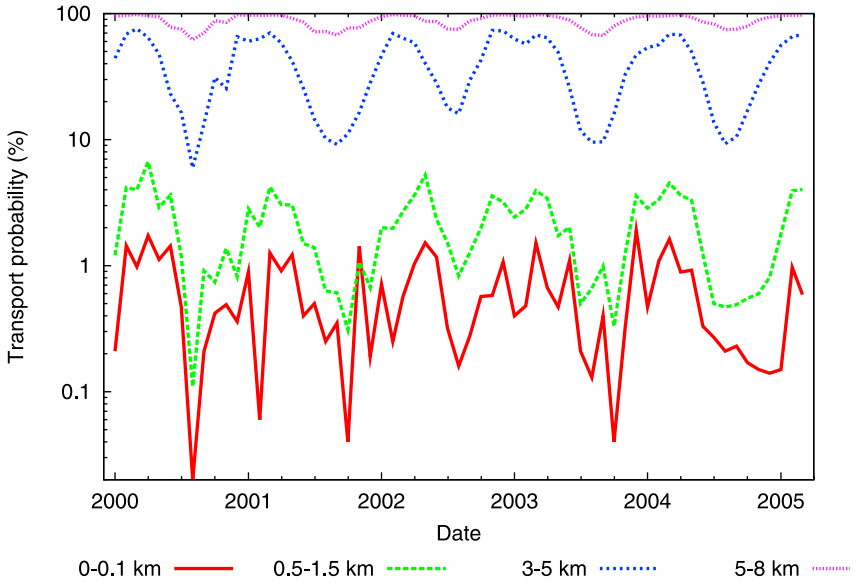

Figure 4. Time series of the monthly mean probability (percentage) that air over the Antarctic Plateau (70°S–86°S, 0°E–141°E) has come from the stratosphere within the last 10 days for four different altitude ranges, where altitudes are given above ground level.

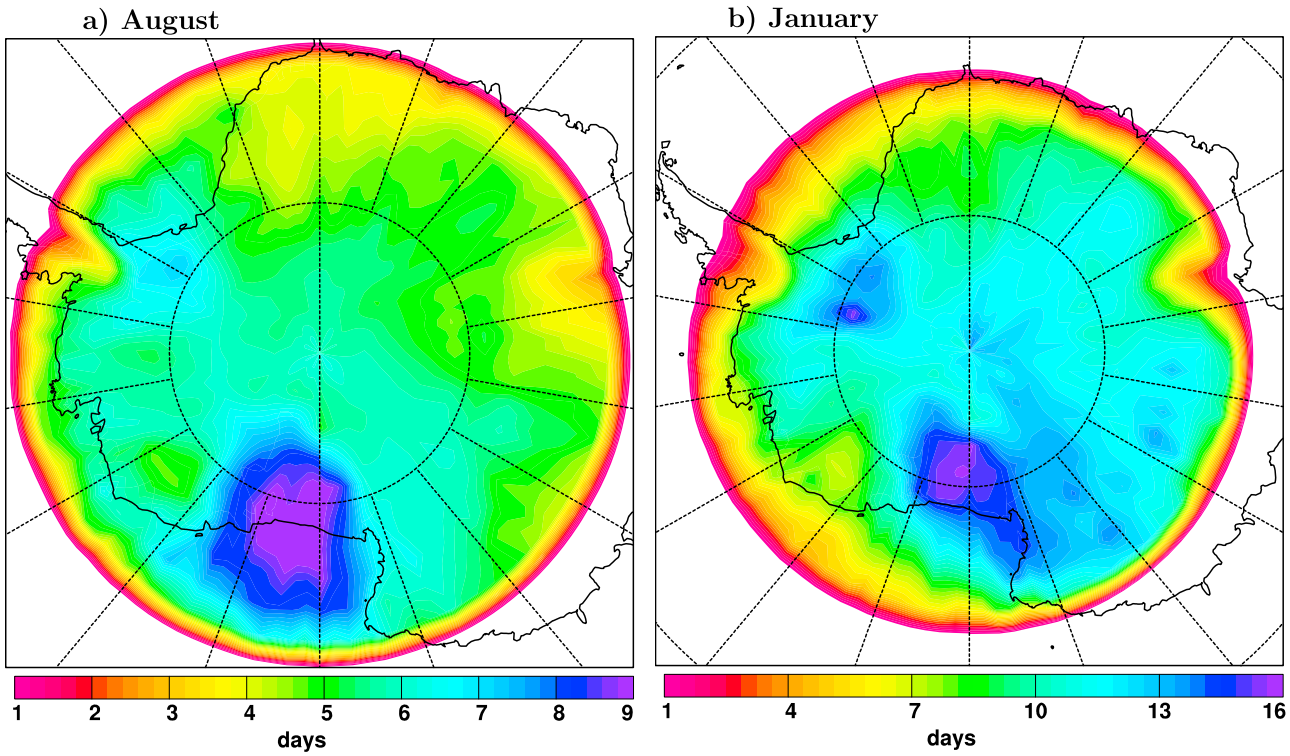

Figure 5. Mean Antarctic age of air in the lowest 100 m of the atmosphere in (a) August and (b) January. Note the different scales.

a winter maximum following the minimum accumulation in winter, the high levels suggest an active injection of tritium from the stratosphere over the Plateau [*Fourré et al.*, 2006].

[19] It is important to notice that the subsidence of stratospheric air to the surface is compatible with atmospheric cooling rates above Antarctica. *Van de Berg et al.* [2007] show time-averaged vertical profiles of the temperature forcing by different mechanisms as obtained from a regional climate model. Over the East Antarctic interior and for winter, they find cooling rates of about minus 2–3 K/d between the surface and about 6 km. The heat loss due to turbulent heat exchange with the surface peaks at −15 K/d close to the surface but is still at about −1 K/d 500 m above. Thus, the potential temperature difference between the surface and the tropopause can easily be overcome on a time scale of 10 days. *Van de Berg et al.* [2007] furthermore show that the heat lost is replaced mainly by the vertical advection term, leading to average subsidence of the order of 5 mm s^{-1}, which would produce a descent of 4.3 km in 10 days, again sufficient to transport air from the height of the tropopause to the top of the inversion layer. Notice that all these values are long-term averages and cooling and subsidence can be stronger. While time-averaged cooling rates and subsidence velocities are smaller in summer [*Van de Berg et al.*, 2007], they are probably still sufficient to bridge the potential temperature difference between the tropopause and the surface. In fall, for which we obtain the largest stratospheric influence near the surface, the cooling rates and subsidence velocities are likely already comparable to those in winter.

3.2. Antarctic Age of Air

[20] Analogous to *Stohl* [2006], we measure the isolation of the Antarctic troposphere from the middle latitudes by the time a particle has spent continuously south of 70 °S: its "Antarctic age." Figure 5 shows the average Antarctic age of air in the lowest 100 m of the atmosphere, for August (Figure 5a) and for January (Figure 5b). While January is clearly the month with the highest Antarctic age of air values, August is representative for a 6 month winter period (May to October) with ∼50% lower values (notice the different scales in Figures 5a and 5b). This is similar to the situation in the Arctic, where transport is slowest and the air is most aged in summer, too. Opposite to what one might expect, the Antarctic age of air does not peak near the South Pole but over the shelf ice regions, especially over the Ross Ice Shelf and the Ronne Ice Shelf where Θ near the surface is lowest (Figure 3). The maximum values found there (9 days in winter and 16 days in summer) are almost as high as the maxima found over the Arctic Ocean [*Stohl*, 2006]. Air entering these regions must be cooled strongly in terms of potential temperature, associated mainly with the katabatic winds. Thus, air in these regions arrives primarily via the continental interior and, thus, has the longest travel times from the middle latitudes. Over the Antarctic Plateau, the average age of air is only 4–6 days in winter and 9–14 days in summer. This implies that the South Pole is more strongly influenced by transport of air from middle latitudes than the North Pole.

[21] In order to measure the isolation of the Antarctic interior from the ocean, we also counted the time since the air was last over water (regardless of altitude, Figure 6), as

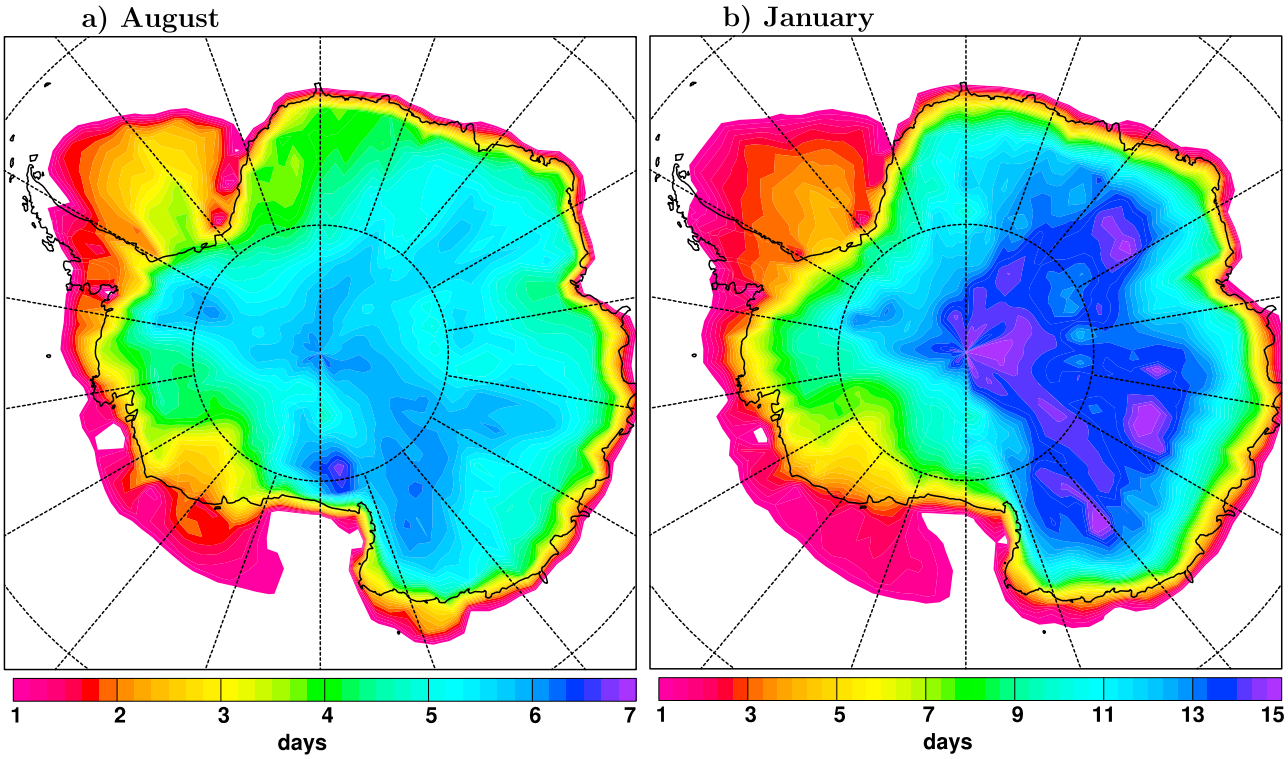

Figure 6. Mean time since air in the lowest 100 m of the Antarctic troposphere was last over open water or seasonal sea ice in (a) August and (b) January.

defined in the land cover data set of *Belward et al.* [1999] resampled to a resolution of 0.3°. As in this data set ice coverage is static at the annual minimum, time was actually counted since an air parcel was either over water or over seasonal sea ice. An important difference to the results for the Antarctic age of air (Figure 5) is that the maxima over the shelf ice regions are absent. Large parts of the Ross Sea near the shelf ice edge are seasonally ice free, providing a short transport route to the ice shelf. In a companion paper, *Sodemann and Stohl* [2009] show that the moisture falling as precipitation in these coastal areas evaporates in the vicinity. Over the Eastern Antarctic interior, the mean times that air has spent away from the ocean (Figure 6) are somewhat longer than the Antarctic age of air (Figure 5). The moisture falling as precipitation in this high-altitude region is transported over long distances from evaporation sources located much further north than for the coastal regions [*Sodemann and Stohl*, 2009] because the coastal air masses are too cold to be lifted isentropically to the Antarctic Plateau. The moisture over the Antarctic Plateau originates over the warmer lower latitude oceans where potential temperatures correspond approximately to those above the Plateau [*Sodemann and Stohl*, 2009], facilitating isentropic transport.

[22] For air near the surface and south of 80°S, we find a consistent seasonal cycle of the mean time air has spent away from the open ocean or seasonal sea ice with a sharp summer maximum of 10–14 days and a broad winter minimum of ~6 days (Figure 7). Notice that transport times from the open ocean (a source, for instance, of sea salt aerosol [*Fischer et al.*, 2007]) can be somewhat longer than indicated here when Antarctica is surrounded by seasonal sea ice in winter. The time scales decrease rapidly with altitude and the seasonal cycle becomes less pronounced in the upper troposphere than near the surface. The same altitude dependence and seasonal variation are found also for the Antarctic age of air (not shown).

3.3. Time in Continuous Darkness and Continuous Sunlight

[23] Light is needed to fuel photolysis reactions and, thus, has a strong influence on chemical processes in the Antarctic troposphere. The duration of the polar day or night at a given location can be calculated from astronomical principles. However, how long an air parcel has been exposed to continuous illumination or continuous darkness depends more on the air parcel's transport than on local light conditions. Therefore, the uninterrupted duration of illumination or darkness for a particle was determined based on hourly calculations of the solar zenith angle at the particle's position.

[24] Figure 8a shows a map of the mean time that air in the lowest 100 m of the atmosphere has spent in darkness for the month with the longest mean times in darkness, July. The patterns found are similar to the Antarctic age of air in August (Figure 5a), with maxima of 11 days over the Ross Ice Shelf and the Ronne Ice Shelf. Air near the South Pole has only spent about 1 week in darkness. In contrast, in the Arctic large regions are covered by air masses having been in darkness for about 2 weeks in December [*Stohl*, 2006, Figure 4].

[25] Exposure to continuous illumination is longest in January (Figure 8b) and peaks at 20 days over the Ross Ice Shelf. It is longer than 2 weeks over most of the Antarctic

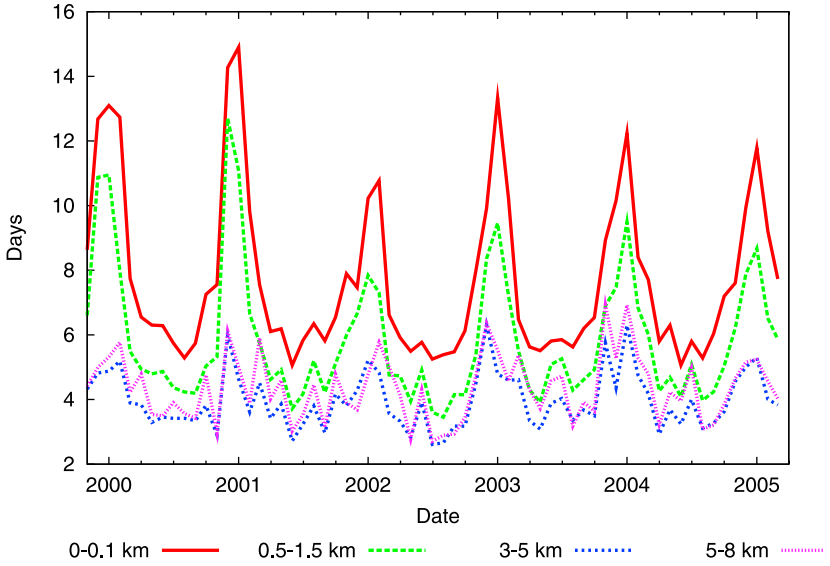

Figure 7. Time series of the mean time air has spent away from the open ocean or seasonal sea ice in the area south of 80°S for four different altitude ranges, where altitudes are given above ground level.

Plateau. As compared to continuous darkness in winter, the duration of continuous illumination in summer maximizes closer to the pole and is weighted more heavily toward eastern Antarctica. This confirms the large potential air over the plateau has for receiving and accumulating nitrogen oxide emissions from the sun-exposed snowpack [*Davis et al.*, 2008] and for subsequent formation of ozone in summer.

3.4. Transport to Antarctica

[26] Here we examine the pathways and time scales of atmospheric transport from lower-latitude regions to Antarctica and characterize the transport potential from Southern Hemisphere pollution source regions. For this, we started by identifying particles that are located south of 70°S for at least 5 consecutive days. This excludes particles just quickly passing through the polar region and leaves particles with a dominately Antarctic character. We used either all particles from the entire Antarctic atmospheric column or, alternatively, only a subset which reached a minimum altitude below 1000 m above sea level (asl). The particles were then tracked back in time for 30 days to calculate a potential emission sensitivity (PES) function for the lowest 500 m of the atmosphere (the so- called footprint) where most emissions take place. The word "potential" shall indicate that transport alone is considered and removal processes, which would decrease the emission sensitivity, are ignored. PES is a measure for the impact a source of unit strength in a given grid cell would have in the Antarctic. Folding PES values with actual emission fluxes taken from an appropriate inventory (see below) yields so-called potential source contributions (PSC), which measure the emissions' impact on Antarctic mixing ratios. Again, the word potential shall indicate that actual source contributions would be lower because of removal processes. Spatial integration of PSC values gives the total simulated mass mixing ratio of the emitted tracer species over Antarctica. For further details on the method, see *Stohl* [2006].

[27] While PES values are independent of emissions, PSC values depend on the actual emission distribution, which is different for every substance. As in the work of *Stohl* [2006], only BC is considered here, which is produced mainly by combustion processes and is particularly important for radiative forcing. BC is taken as a surrogate for many other species that are also emitted by combustion processes. Temporally constant combined fossil fuel and biofuel BC emissions were taken from the inventory of *Bond et al.* [2007] for the year 2000 (Figure 9, top). Biomass burning BC emissions were based on the RETRO data set [*Schultz et al.*, 2008] (Figure 9, bottom). The RETRO inventory ignores agricultural fires and has ~20% lower emissions than another inventory by *Bond et al.* [2004] but it has the advantage of monthly resolution, from which seasonal mean emissions were calculated using data for the years 1991–2000. Biomass burning is at maximum during spring in South America and Australia, and during winter in Southern Africa.

3.4.1. Winter

[28] At 3 days back in time before entering the Antarctic at 70°S (Figure 10, top left), a small fraction of particles tracked back from the entire Antarctic column has reentered from the Antarctic but most of the particles come from north of 70°S. PES values over all continents other than Antarctica are still close to zero, except for the southern tip of South America. There is a preferred pathway of air into the Antarctic from the eastern half of the South Pacific Ocean with surface contact over the Amundsen and Bellingshausen Seas. This pathway follows approximately the Antarctic Polar Front which is located furthest south near the longitudes of the Antarctic Peninsula. On the other hand, there is relatively little surface contact over the Indian Ocean where the Antarctic Polar Front is located far north. These zonal asymmetries of transport are, however, much smaller than for the Arctic [*Stohl*, 2006, Figure 8].

[29] Integrating back in time over the typical aerosol lifetime of 10 days (Figure 10, middle left), emission sensitivity has spread further north and substantial PES values can be found over the southern parts of South America, Australia and Africa. Nevertheless, an emission

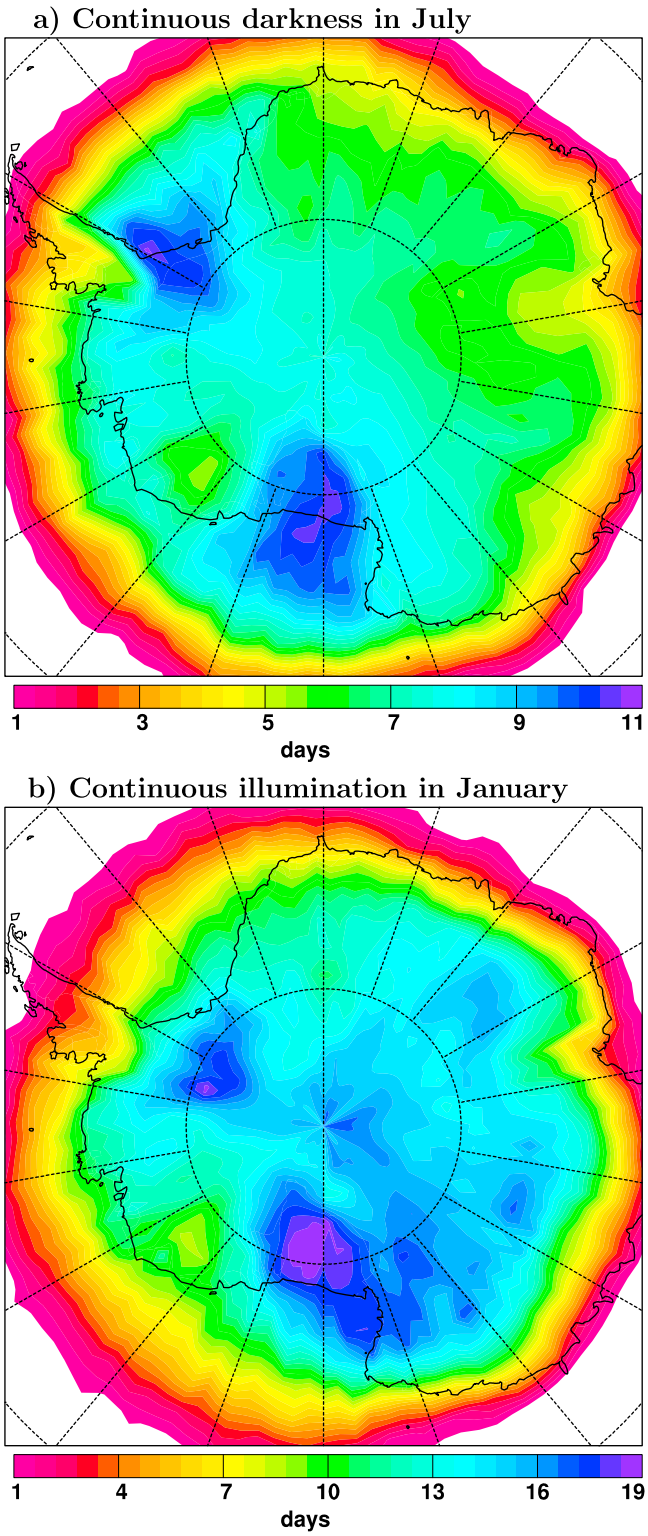

Figure 8. Mean time in days that air in the lowest 100 m has spent in continuous (a) darkness in July and (b) illumination in January.

source at the southern tip of these continents would have to be 2–3 orders of magnitude stronger than an emission source for instance in the Amundsen Sea to cause the same impact on Antarctic aerosol concentration levels. This clearly has implications for the increasing emissions in and around Antarctica and we will come back to this issue in section 3.4.3.

[30] Integrating over 30 days back in time (Figure 10, bottom left), PES fields are homogeneous over the Southern Ocean, whereas continental influence is still strongest over the southern parts of the continents. For instance, an emission source in northern Australia would have to be 2–3 orders of magnitude stronger than an emission source in southern Australia to impact Antarctica equally strong on a 30 day time scale. Meridional differences over the other continents are even larger. For the subset of particles reaching minimum altitudes below 1000 m asl south of 70°S, we only show a PES map integrated over 30 days (Figure 11, left). It is generally similar to the PES map for the full set of particles (Figure 10, bottom left), except that meridional gradients are stronger and, thus, sources close to the Antarctic continent are even more important.

[31] A comparison to the Arctic [*Stohl*, 2006] shows that for transport to the Antarctic on the 10 day time scale the largest PES values over South America, Africa and Australia are 1–2 orders of magnitude smaller than over Eurasia for transport to the Arctic. Thus, already from this simple analysis it is clear that continental emissions have a much smaller impact on the concentrations of short-lived tracers for the Antarctic than for the Arctic. This is not because of a specific transport barrier (in section 3.2 we have shown that transport within the polar region is actually faster for the Antarctic than for the Arctic) but simply because continents are located further away from the pole and meridional distance is the most important parameter determining emission sensitivity in both hemispheres.

[32] Folding the PES values with BC emission fluxes yields potential source contributions (PSC), shown in Figure 12 for the subset of particles reaching a minimum altitude below 1000 m asl and for the full 30 day period of tracking, for anthropogenic and biomass burning BC emissions separately. As a result of the strong meridional gradient of the PES distribution, PSCs are concentrated near the southern parts of the continents, even though emission fluxes (Figure 9) are often higher further north. Overall, biomass burning emissions cause a higher total PSC than anthropogenic emissions (8.8 pptm versus 6.3 pptm) because of larger biomass burning than anthropogenic contributions from Australia and Africa. Coincidentally, the total PSC from South America, Africa and Australia differ from each other by only about a factor of 2 (both for anthropogenic and biomass burning emissions), despite the order of magnitude difference in continental total emissions (Figure 9). Africa, which has the highest total emissions, makes the smallest PSC, a result of its location relatively far north. Australia, which has the lowest total emissions makes a disproportionally large PSC because of relatively large emissions near its southern coast. Similarly, New Zealand also contributes substantially to anthropogenic BC over Antarctica. Also visible in Figure 12a are PSC from the Southern Ocean along the major ship routes to Antarctica, for instance near the tip of the Antarctic peninsula, or south of Australia. However, notice that ship emissions near Antarctica are actually concentrated in summer, which is not reflected in our annual inventory. The local ship emissions will be discussed in more detail in section 3.4.3.

[33] The total anthropogenic PSC for the Antarctic, 6.3 pptm, is small compared to the corresponding value, 175 pptm, for the Arctic [*Stohl*, 2006, Figure 10], even for the relatively long 30 day tracking time. This underlines the smaller potential for pollution to reach the Antarctic than to reach the Arctic.

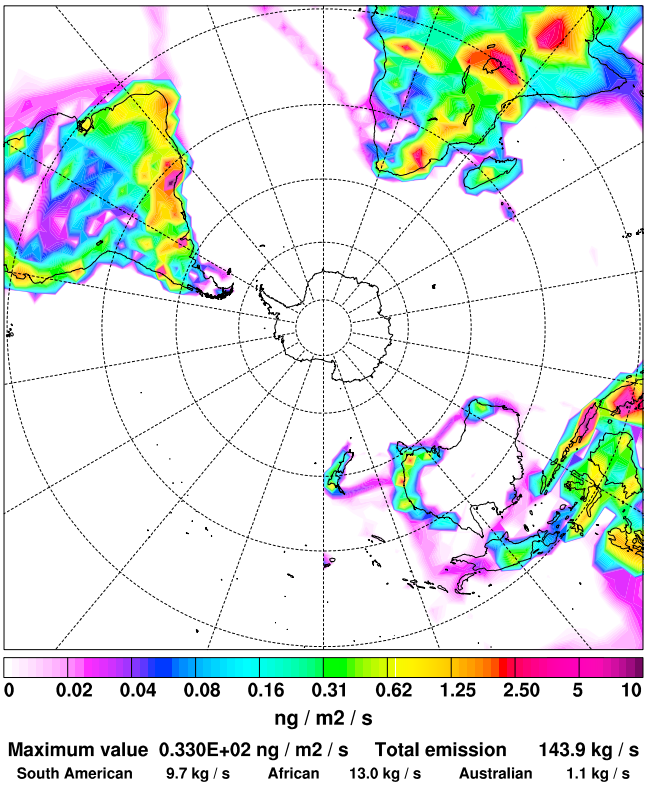

Figure 9. Annual mean BC emissions from fossil fuel and biofuel combustion taken from (top) the inventory of *Bond et al.* [2007] and (bottom) from wildland fires taken from the RETRO inventory [*Schultz et al.*, 2008], remapped to 2° × 3° resolution. Below each plot, the maximum field value, the globally integrated emission flux, and the emission fluxes integrated over the regions of South America, Africa, and Australia are listed. Notice that biomass burning emissions have a strong seasonality (not shown) with peaks in winter (southern Africa) or spring (South America, Australia).

[34] Figure 13 shows the BC PSC from the different continents as a function of time back since the crossing of 70°S. PSC generally increases rapidly with travel time. Consequently, for travel times typical of aerosol lifetimes (5–10 days), PSC values are much smaller than for the 30 days shown in Figure 12 and they are also concentrated more strongly toward the high southern latitudes (not shown). The very small PSC values for short travel times explain why haze is normally not formed in the Antarctic. For the Arctic, PSC from Europe is substantial already for travel times of a few days only [*Stohl*, 2006, Figure 11] and, thus, aerosols can reach the Arctic, causing Arctic Haze. The PSC growth is also different for the different source regions and source types. For instance, South American fires contribute very little to the total PSC at travel times of a few days but become comparable to the largest other sources at a travel time of 30 days. This is a consequence of the large fire emissions which are, however, located relatively far north (Figure 9).

[35] The continental PSC is generally similar for the total Antarctic air column (Figure 13, top) and the low-altitude subset (Figure 13, bottom) but there are also important differences. For instance, for travel times of 5 days or less, South American anthropogenic emissions are more important near the surface than for the entire atmospheric column, a consequence of occasional rapid low-level transport from the southern parts of South America to the Antarctic Peninsula [*Pereira et al.*, 2006]. In contrast, emissions from South American fires are more important at higher altitudes.

3.4.2. Summer

[36] In summer, the meridional circulation at middle latitudes is less vigorous than in winter. Consequently, in summer PES values are higher near the Antarctic continent and lower over foreign continents than in winter. This is true both for the particles tracked from the entire Antarctic column (Figure 10) as well as for the subset of low-altitude particles (Figure 11). Compared to the winter situation, the main entrance region of midlatitude air is shifted toward the Antarctic Peninsula in summer (Figure 10, top right). This favors transport of air from South America, leading to only slightly lower PES values over that continent compared to winter, especially for the shorter time scales (Figure 10, top and middle right). PES values over Africa are much more strongly reduced compared to winter. For example, at the 10 day time scale, PES values are still close to zero over Africa (Figure 10, middle right). This is in good agreement with studies by *Krinner and Genthon* [2003] and *Li et al.* [2008], which showed that transport from South America

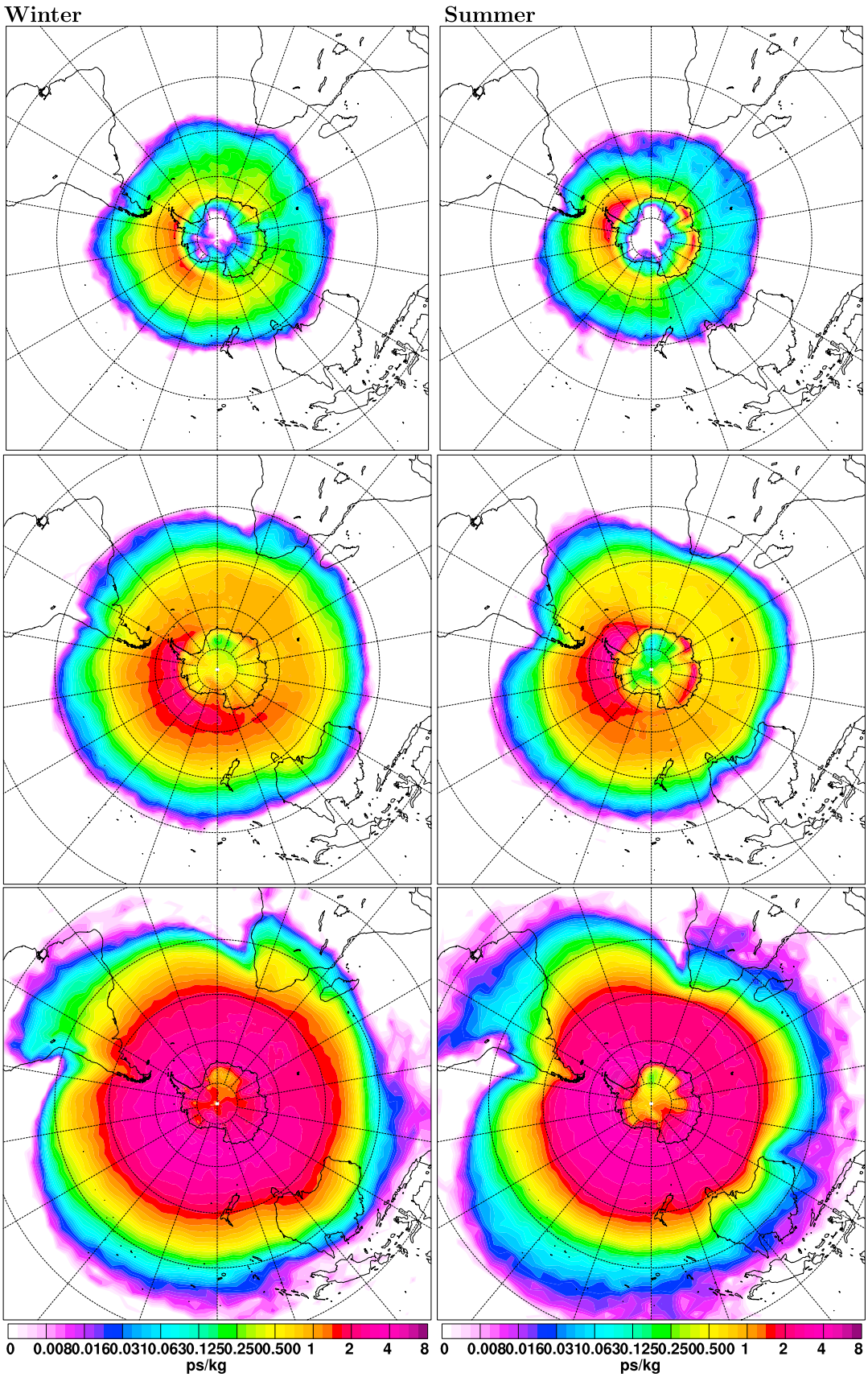

Figure 10. PES for air that spends at least 5 days in the Antarctic, integrated over the last (top) 3 days, (middle) 10 days, and (bottom) 30 days before it arrived in the Antarctic, for winter (June, July, August, shown at left) and summer (December, January, February, shown at right).

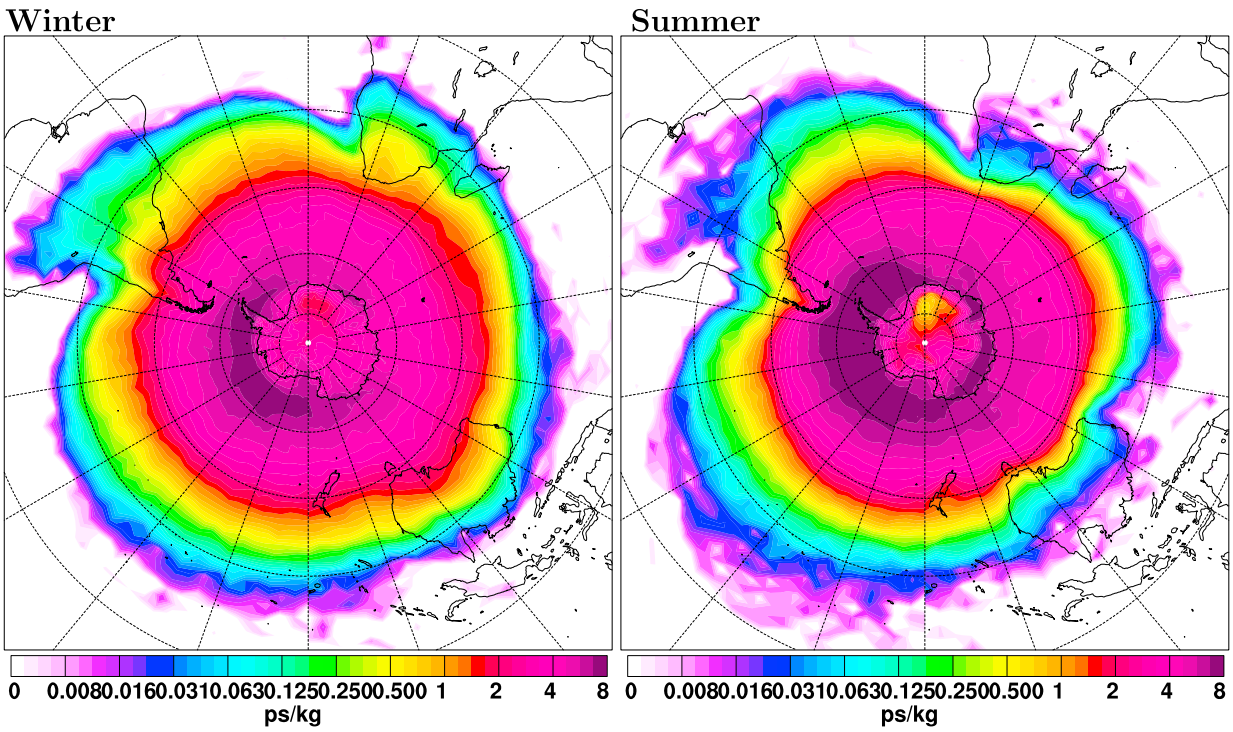

Figure 11. PES for air that spends at least 5 days in the Antarctic and reaches a minimum Antarctic altitude below 1000 m above sea level (asl), integrated over the last 30 days before it arrived in the Antarctic, for (left) winter and (right) summer.

to Antarctica is fastest, while transport from Africa to Antarctica is slowest.

[37] As a consequence of reduced PES values, total anthropogenic PSC for the 30 day time scale is only 2.3 pptm in summer (Figure 12b), compared to 6.3 pptm in winter (Figure 12a). The relative reduction is largest for Africa (0.1 pptm compared to 1.0 pptm) and smallest for South America. Overall, South American anthropogenic BC PSC dominates all other sources, both for the total column (Figure 14, top) and even more so for the near-surface air (Figure 14, bottom). The relative contribution of South America is largest for the shortest time scales.

[38] The reduction of PES in the middle latitudes in summer compared to winter is similar to the situation in the Arctic. The resulting relative decrease in total anthropogenic BC PSC in summer is ~60% for both polar regions. However, while there is active biomass burning at high northern latitudes in summer [*Stohl*, 2006, Figure 16], biomass burning in the southerly parts of the Southern Hemisphere continents is higher in winter. Consequently, the total biomass burning BC PSC for the Antarctic is more than an order of magnitude smaller in summer than in winter (0.6 pptm compared to 8.8 pptm, see Figures 12c and 12d), the combined effect of smaller emissions and slower transport. Almost all the biomass burning influence in summer comes from Australia.

3.4.3. The Importance of Local Sources

[39] Local pollution sources are strongly increasing in Antarctica, due to increased research activity but especially because of a rising number of tourists. While 6000 tourists have visited Antarctica (mostly with ships) in 1992–1993, this number was up to 26000 in 2005–2006 [*Shirsat and Graf*, 2009]. Half of the annual tourist activity occurs in a single month, December [*Shirsat and Graf*, 2009]. This activity appears to be reflected in the *Bond et al.* [2007] emission inventory, with annual BC emissions south of 60°S of 100 Mg. Converting the sulfur dioxide emissions reported for Antarctica by *Shirsat and Graf* [2009] to BC emissions using typical emission ratios for shipping, we obtain an annual BC emission of the order of only 20 Mg. However, *Shirsat and Graf* [2009] did not account for fishing, which is also an important activity in the seas surrounding Antarctica.

[40] Using the emission inventory of *Bond et al.* [2007] and assuming that half of the annual emissions south of 60°S occur in December while anthropogenic BC emissions are temporally constant elsewhere, we calculated PSC for the Antarctic air in the lowest 1000 m asl. For time scales of 5, 10, and 30 days, PSC values from south of 60°S are 0.06, 0.10 and 0.16 pptm, compared to total PSC values of 0.1, 0.27 and 2.3 pptm. For the shorter time scales of 5 and 10 days which can be considered as typical aerosol lifetimes, the region south of 60°S thus contributes 40–60% of the total PSC in December. This fraction would increase by taking into account the probably longer lifetime of aerosols emitted in the Antarctic compared to those emitted further north. Our calculations are averages over all of Antarctica. Regionally, BC mixing ratios could reach much higher levels, for instance near the Antarctic Peninsula where most of the tourist activity occurs.

[41] While the simulated BC mixing ratios are very low compared to the Arctic, this is nevertheless a matter of concern. BC emissions are accompanied by emissions of heavy metals, polycyclic aromatic hydrocarbons and other

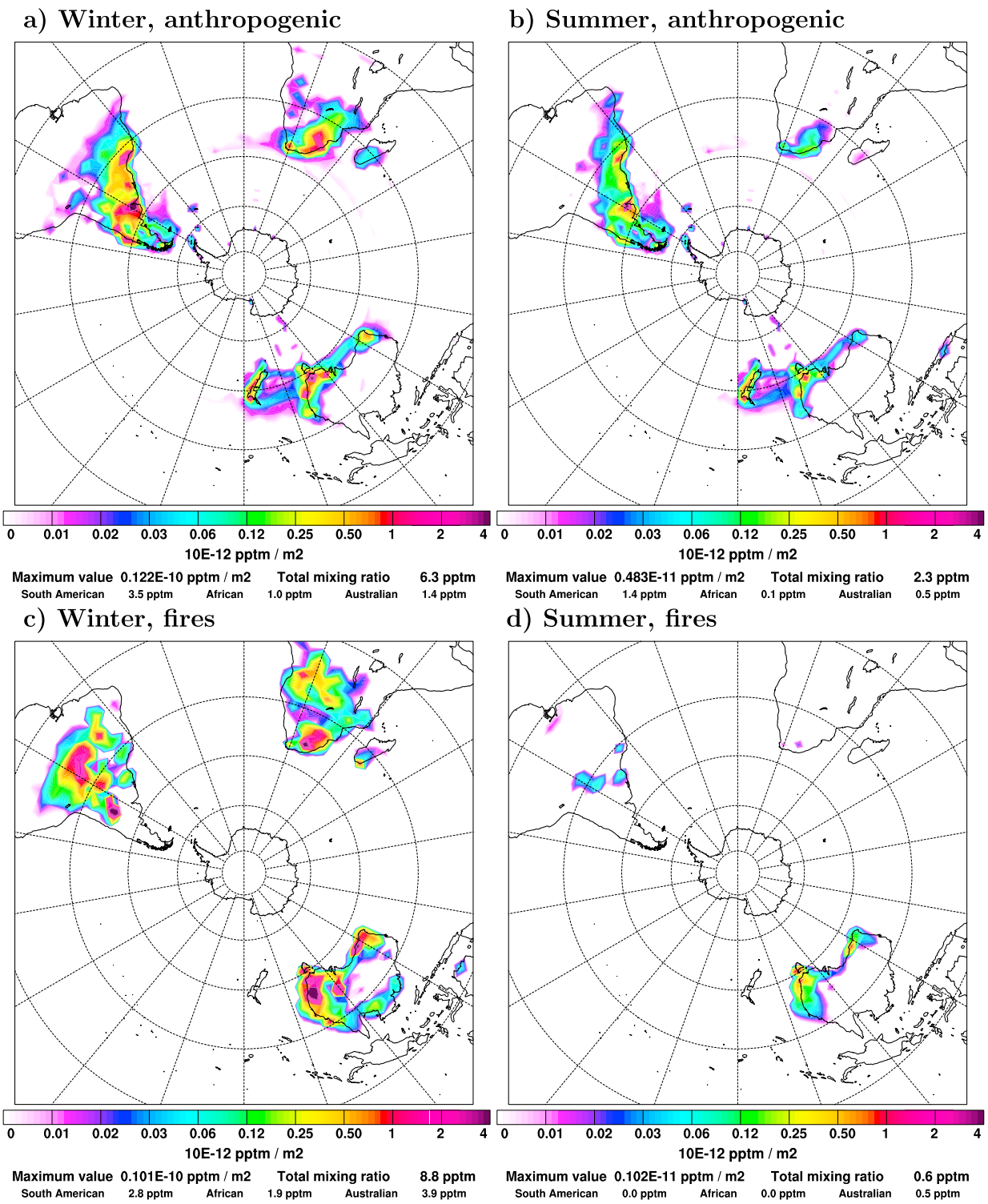

Figure 12. BC PSC maps for a travel time of 30 days for particles that spend at least 5 days in the Antarctic while reaching a minumum altitude below 1000 m asl, (a) for anthropogenic emissions in winter, (b) for anthropogenic emissions in summer, (c) for biomass burning emissions in winter, and (d) for biomass burning emissions in summer. At the bottom of each plot, the total mixing ratio as well as the contributions from the Southern Hemisphere continents are reported.

toxic compounds, and these may have nonnegligible impacts on the fragile Antarctic ecosystems. If Antarctica is to be preserved in its natural state, pollution impact is to be kept minimal. According to our results, controlling local emissions is essential to achieve this goal, especially in the face of increasing human presence in Antarctica. This calls for a careful monitoring of pollution trends, use of clean technology for ships visiting Antarctica, and a strict

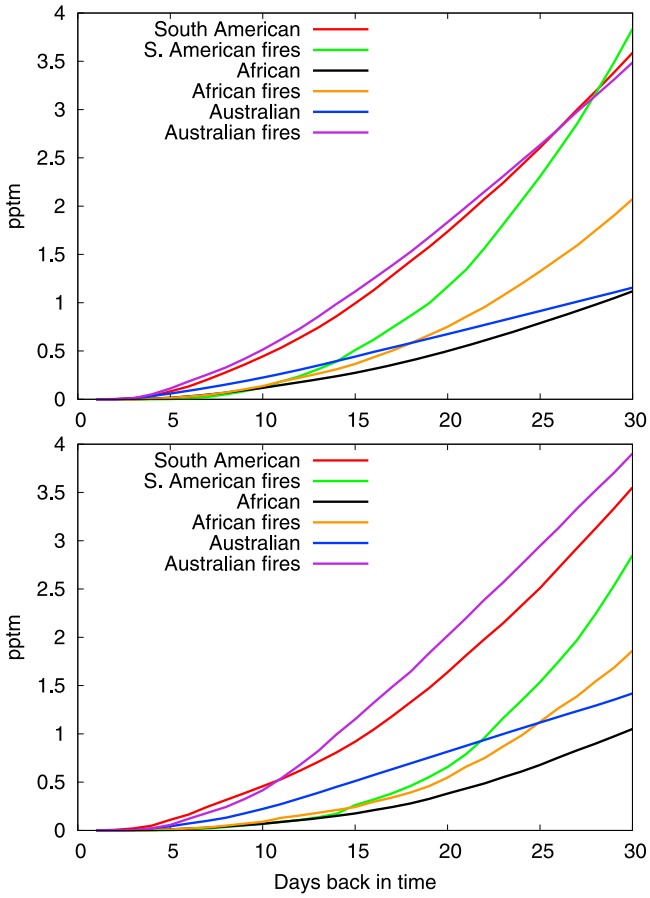

Figure 13. BC PSCs from different continents and source types as a function of transport time to the Antarctic, (top) for particles that spend at least 5 days in the Antarctic and (bottom) for the subset that also reaches a minimum Antarctic altitude below 1000 m, for winter.

limitation of the number of visiting people. Similarly, emissions from fishing vessels operating in the seas surrounding Antarctica should also be subject to emission regulations and monitoring.

4. Conclusions

[42] In this paper, we have used a Lagrangian particle dispersion model, FLEXPART, to study transport into the Antarctic troposphere. Using 6 hourly particle position output, certain transport-related time scales (e.g., time in darkness) and properties (e.g., probability of transport from the stratosphere) have been calculated. Under the assumption that loss processes can be ignored, potential emission sensitivities were derived for time scales up to 30 days. On the basis of these emission sensitivities, potential source contributions were calculated at the example of BC using inventories for anthropogenic and biomass burning emissions. Ignoring loss processes certainly affects our capability to quantitatively simulate BC transport. Our aim here was mainly to characterize the pathways and time scales of the transport, and BC was only taken as an example. Our results are equally valid for other substances with similar source distributions (e.g., combustion products; in a broader sense most substances emitted on Southern Hemisphere continents). By choosing a transport time scale comparable to the typical lifetime of a substance, approximate source contributions from different regions can be derived from our results.

[43] Our conclusions from this study are as follows:

[44] 1. Stratospheric air is brought down into the lower troposphere by descending air masses above the Antarctic continent. The probability that air near the surface of the Antarctic Plateau has come from the stratosphere within 10 days is ~0.7% (2%) in spring (fall). This is almost an order of magnitude greater than corresponding values near the North Pole. Lower transport probabilities, comparable to Arctic values, are found in a zonal band around Antarctica and especially over the Ronne Ice Shelf and Ross Ice Shelf regions. The seasonality of transport from the stratosphere with a maximum in late summer and a minimum in late winter is contrary to that in the Arctic.

[45] 2. The average time for which air near the surface has been exposed to continuous darkness in July (continuous light in January) is longest over the Ronne Ice Shelf and Ross Ice Shelf at ~11 days (20 days). The time air has been in complete darkness near the South Pole in July, about a week, is only half as long as the corresponding value near the North Pole.

[46] 3. The average time air near the surface of the Antarctic Plateau has spent continuously south of 70°S is 4–6 days in summer and 9–14 days in winter. Average

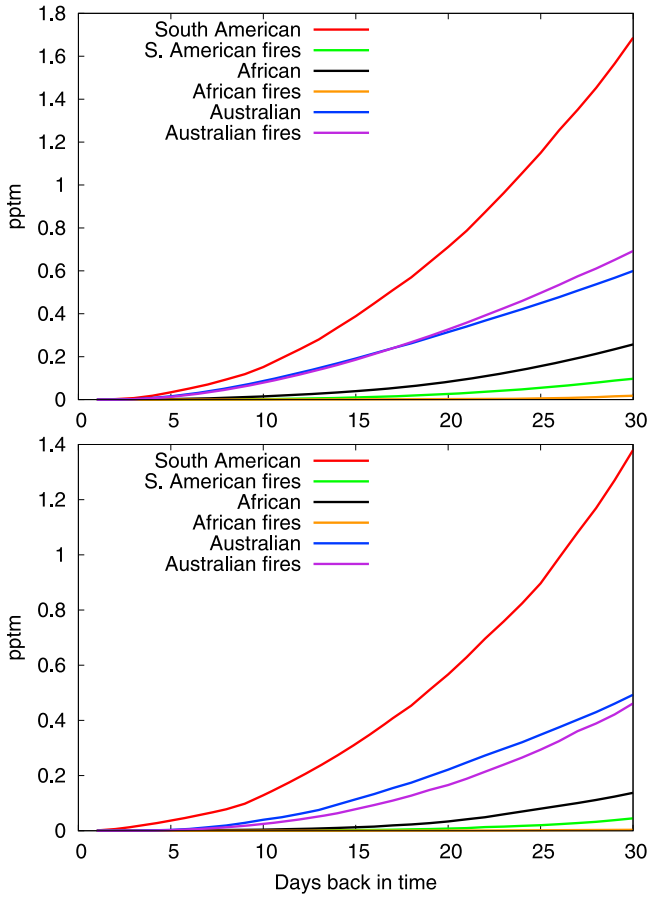

Figure 14. Same as Figure 13, but for summer.

times that air has spent away from the ocean are somewhat longer, and average times for both quantities decrease strongly with altitude. This means that the Antarctic is relatively well connected to the middle latitudes and near-surface air near the South Pole is more influenced by atmospheric transport from the middle latitudes than air near the North Pole.

[47] 4. To determine in which regions emissions can influence Antarctic atmospheric composition, we calculated potential emission sensitivity (PES) values as a function of time, ignoring loss processes. On all time scales, meridional gradients of PES fields are very strong. On the 10 day time scale, in winter PES values near the southern ends of South America, Africa or Australia are 2–3 orders of magnitude lower than over the Amundsen Sea. On the 30 day time scale, emission sensitivity in northern Australia is 2–3 orders of magnitude lower than in southern Australia. Thus, while air above Antarctica is well connected to the middle latitudes, the long distance to the continents makes it unlikely for air from these continents to reach Antarctica on time scales relevant for aerosols and many short-lived trace gases.

[48] 5. By folding PES values with BC emission fluxes, potential source contributions (PSC) were calculated. In winter, biomass burning and anthropogenic emissions contribute 8.8 pptm and 6.3 pptv BC to Antarctic air on the 30 day time scale, respectively. The largest individual contributions come from Australian and South American fires (3.9 pptm and 2.8 pptm, respectively), and South American anthropogenic sources (3.5 pptm). Africa, which has the highest total emissions of the Southern Hemisphere continents, makes a relatively small contribution, because emissions are located further north than over South America and Australia. Australia, which has relatively small total emissions, makes a relatively large contribution because a large fraction of its emissions is located near its south coast.

[49] 6. Comparing the winter situation in the Antarctic and in the Arctic, we find that for the 10 day time scale, the largest PES values over South America, Africa and Australia are 1–2 orders of magnitude smaller than over Eurasia for transport to the Arctic. Consequently, PSC for the Antarctic are much smaller than for the Arctic. Even for the 30 day time scale, the anthropogenic contribution to the Antarctic (6.3 pptm) is nearly a factor of 30 smaller than the anthropogenic contribution to the Arctic (175 pptm). Relative differences are even larger for shorter time scales.

[50] 7. In summer, PES values near Antarctica are higher while PES values over other continents are smaller than in winter. Over Africa, for instance, there is a factor 10 reduction in BC PSC, even on the 30 day time scale. Thus, PSC values are very low in summer: 2.3 pptm and 0.6 pptm for anthropogenic sources and biomass burning, respectively.

[51] 8. For typical aerosol lifetimes of 5–10 days, BC emissions from ships operating south of 60°S (as contained in the *Bond et al.* [2007] inventory) were found to account for 40–60% of the total BC PSC in December, considering the entire Antarctic region below 1000 m asl. Regionally, and especially for the Antarctic Peninsula, ships are likely to be the dominant source of BC and other pollutants in Antarctica during summer. This makes the recent dramatic increase in the number of tourists visiting Antarctica, as well as fishing activities at high southern latitudes a matter of concern.

[52] **Acknowledgments.** We appreciate the many comments provided by three reviewers, which helped us improve this manuscript. We thank ECMWF and met.no for access to the ECMWF archives. Funding for this study was provided by the Norwegian Research Council in the framework of POLARCAT and CLIMSLIP.

References

Arimoto, R., T. Zeng, D. Davis, Y. Want, H. Khaing, C. Nesbit, and G. Huey (2008), Concentrations and sources of aerosol ions and trace elements during ANTCI-2003, *Atmos. Environ.*, *42*, 2864–2876.

Belward, A. S., J. E. Estes, and K. D. Kline (1999), The IGBP-DIS global 1-km land-cover data set DISCover: A project overview, *Photogramm. Eng. Remote Sens.*, *65*, 1013–1020.

Bond, T. C., D. G. Streets, K. F. Yarber, S. M. Nelson, J.-H. Woo, and Z. Klimont (2004), A technology-based global inventory of black and organic carbon emissions from combustion, *J. Geophys. Res.*, *109*, D14203, doi:10.1029/2003JD003697.

Bond, T. C., E. Bhardwaj, R. Dong, R. Jogani, S. Jung, C. Roden, D. G. Streets, S. Fernandes, and N. Trautmann (2007), Historical emissions of black and organic carbon aerosol from energy-related combustion, 1850–2000, *Global Biogeochem. Cycles*, *21*, GB2018, doi:10.1029/2006GB002840.

Carrasco, J. F., and D. H. Bromwich (1994), Climatological aspects of mesoscale cyclogenesis over the Ross Sea and Ross Ice Shelf regions of Antarctica, *Mon. Weather Rev.*, *122*, 2405–2425.

Connolley, W. M. (1996), The Antarctic temperature inversion, *Int. J. Climatol.*, *16*, 1333–1342.

Court, A. (1942), Tropopause disappearance during the Antarctic winter, *Bull. Am. Meteorol. Soc.*, *23*, 220–238.

Dalu, G. A., M. Baldi, M. D. Moran, C. Nardone, and L. Sbano (1993), Climatic atmospheric outflow at the rim of the Antarctic continent, *J. Geophys. Res.*, *98*, 12,955–12,960.

Davis, D. D., et al. (2008), A reassessment of Antarctic plateau reactive nitrogen based on ANTCI 2003 airborne and ground based measurements, *Atmos. Environ.*, *42*, 2831–2848.

Delmonte, B., I. Basile-Doelsch, J.-R. Petit, V. Maggi, M. Revel-Rolland, A. Michard, E. Jagoutz, and F. Grousset (2004), Comparing the Epica and Vostok dust records during the last 220,000 years: Stratigraphical correlation and provenance in glacial periods, *Earth Sci. Rev.*, *66*, 63–87.

Eckhardt, S., A. Stohl, H. Wernli, P. James, C. Forster, and N. Spichtinger (2004), A 15-year climatology of warm conveyor belts, *J. Clim.*, *17*, 218–237.

Emanuel, K. A., and M. Živković-Rothman (1999), Development and evaluation of a convection scheme for use in climate models, *J. Atmos. Sci.*, *56*, 1766–1782.

Evangelista, H., et al. (2007), Sources and transport of urban and biomass burning aerosol black carbon at the South-West Atlantic coast, *J. Atmos. Chem.*, *56*, 225–238.

Fiebig, M., C. R. Lunder, and A. Stohl (2009), Tracing biomass burning aerosol from South America to Troll research station, Antarctica, *Geophys. Res. Lett.*, *36*, L14815, doi:10.1029/2009GL038531.

Fischer, H., M.-L. Siggaard-Andersen, U. Ruth, R. Röthlisberger, and E. Wolff (2007), Glacial/interglacial changes in mineral dust and sea-salt records in polar ice cores: Sources, transport, and deposition, *Rev. Geophys.*, *45*, RG1002, doi:10.1029/2005RG000192.

Forster, C., A. Stohl, and P. Seibert (2007), Parameterization of convective transport in a Lagrangian particle dispersion model and its evaluation, *J. Appl. Meteorol. Climatol.*, *46*, 403–422.

Fourré, E., P. Jean-Baptiste, A. Dapoigny, D. Baumier, J.-R. Petit, and J. Jouzel (2006), Past and recent tritium levels in Arctic and Antarctic polar caps, *Earth Planet. Sci. Lett.*, *245*, 56–64.

Gasso, S., and A. F. Stein (2007), Does dust from Patagonia reach the sub-Antarctic Atlantic Ocean?, *Geophys. Res. Lett.*, *34*, L01801, doi:10.1029/2006GL027693.

Helmig, D., S. J. Oltmans, D. Carlson, J.-F. Lamarque, A. Jones, C. Labuschagne, K. Anlauf, and K. Hayden (2007), A review of surface ozone in the polar regions, *Atmos. Environ.*, *41*, 5138–5161.

Helsen, M. M., R. S. W. van de Wal, M. R. van den Broeke, V. Masson-Delmotte, H. A. J. Meijer, M. P. Scheele, and M. Werner (2006), Modeling the isotopic composition of Antarctic snow using backward trajectories: Simulation of snow pit records, *J. Geophys. Res.*, *111*, D15109, doi:10.1029/2005JD006524.

Hogan, A., S. Barnard, J. Samson, and W. Winters (1982), The transport of heat, water vapor and particulate material to the South Polar Plateau, *J. Geophys. Res.*, *87*, 4287–4292.

James, I. N. (1989), The Antarctic drainage flow: Implications for hemispheric flow on the Southern Hemisphere, *Antarctic Sci.*, *1*, 279–290.
James, P., A. Stohl, C. Forster, S. Eckhardt, P. Seibert, and A. Frank (2003), A 15-year climatology of stratosphere-troposphere exchange with a Lagrangian particle dispersion model: 2. Mean climate and seasonal variability, *J. Geophys. Res.*, *108*(D12), 8522, doi:10.1029/2002JD002639.
Kottmeier, C., and B. Fay (1998), Trajectories in the Antarctic lower troposphere, *J. Geophys. Res.*, *103*, 10,947–10,959.
Krinner, G., and C. Genthon (2003), Tropospheric transport of continental tracers toward Antarctica under varying climatic conditions, *Tellus, Ser. B*, *55*, 54–70.
Li, F., P. Ginoux, and V. Ramaswamy (2008), Distribution, transport, and deposition of mineral dust in the Southern Ocean and Antarctica: Contribution of major sources, *J. Geophys. Res.*, *113*, D10207, doi:10.1029/2007JD009190.
Massom, R. A., M. J. Pook, J. C. Comiso, N. Adams, J. Turner, T. Lachlan-Cope, and T. T. Gibson (2004), Precipitation over the interior East Antarctic ice sheet related to midlatitude blocking-high activity, *J. Clim.*, *17*, 1914–1928.
McConnell, J. R., A. J. Aristarain, J. R. Banta, P. R. Edwards, and J. C. Simões (2007), 20th-century doubling in dust archived in an Antarctic Peninsula ice core parallels climate change and desertification in South America, *Proc. Natl. Acad. Sci. U. S. A.*, *104*, 5743–5748.
Minikin, A., M. Legrand, J. Hall, D. Wagenbach, C. Kleefeld, E. Wolff, E. C. Pasteur, and D. Ducroz (1998), *J. Geophys. Res.*, *103*, 10,975–10,990.
Murphey, B. B., and A. W. Hogan (1992), Meteorological transport of continental soot to Antarctica?, *Geophys. Res. Lett.*, *19*, 33–36.
Neff, W. D. (1999), Decadal timescale trends and variability in the tropospheric circulation over the South Pole, *J. Geophys. Res.*, *104*, 27,217–27,251.
Parish, T. R., and D. H. Bromwich (2007), Reexamination of the near-surface airflow over the Antarctic continent and implications on atmospheric circulations at high southern latitudes, *Mon. Weather Rev.*, *135*, 1961–1973.
Pereira, E. B., H. Evangelista, K. C. D. Pereira, I. F. A. Cavalcanti, and A. W. Setzer (2006), Apportionment of black carbon in the South Shetland Islands, Antarctic Peninsula, *J. Geophys. Res.*, *111*, D03303, doi:10.1029/2005JD006086.
Quinn, P. K., et al. (2008), Short-lived pollutants in the Arctic: Their climate impact and possible mitigation strategies, *Atmos. Chem. Phys.*, *8*, 1723–1735.
Reijmer, C. H., M. R. van den Broeke, and M. P. Scheele (2002), Air parcel trajectories and snowfall related to five deep drilling locations in Antarctica based on the ERA-15 dataset, *J. Clim.*, *15*, 1957–1968.
Revel-Rolland, M., P. de Deckker, B. Delmonte, P. P. Hesse, J. W. Magee, I. Basile-Doelsch, F. Grousset, and D. Bosch (2006), Eastern Australia: A possible source of dust in East Antarctica interglacial ice, *Earth Planet. Sci. Lett.*, *249*, 1–13.
Roscoe, H. K. (2004), Possible descent across the "tropopause" in Antarctic winter, *Adv. Space Res.*, *33*, 1048–1052.
Savoie, D. L., J. M. Prospero, R. J. Larsen, and E. S. Saltzman (1992), Nitrogen and sulfur species in aerosols at Mawson, Antarctica, and their relationship to natural radionuclides, *J. Atmos. Chem.*, *14*, 181–204.
Schlosser, E., O. H. Oerter, V. Masson-Delmotte, and C. Reijmer (2008), Atmospheric influence on the deuterium excess signal in polar firn: Implications for ice core interpretation, *J. Glaciol.*, *54*, 117–124.
Schultz, M. G., A. Heil, J. J. Hoelzemann, A. Spessa, K. Thonicke, J. G. Goldammer, A. C. Held, J. M. C. Pereira, and M. van het Bolscher (2008), Global wildland fire emissions from 1960 to 2000, *Global Biogeochem. Cycles*, *22*, GB2002, doi:10.1029/2007GB003031.
Shirsat, S., and H. Graf (2009), An emission inventory of sulfur from anthropogenic sources in Antarctica, *Atmos. Chem. Phys.*, *9*, 3397–3408.
Simmonds, I., K. Keay, and E. P. Lim (2003), Synoptic activity in the seas around Antarctica, *Mon. Weather Rev.*, *131*, 272–288.
Sodemann, H., and A. Stohl (2009), Asymmetries in the moisture origin of Antarctic precipitation, *Geophys. Res. Lett.*, *36*, L22803, doi:10.1029/2009GL040242.
Stohl, A. (2006), Characteristics of atmospheric transport into the Arctic troposphere, *J. Geophys. Res.*, *111*, D11306, doi:10.1029/2005JD006888.
Stohl, A., and D. J. Thomson (1999), A density correction for Lagrangian particle dispersion models, *Boundary Layer Meteorol.*, *90*, 155–167.
Stohl, A., M. Hittenberger, and G. Wotawa (1998), Validation of the Lagrangian particle dispersion model FLEXPART against large scale tracer experiment data, *Atmos. Environ.*, *32*, 4245–4264.
Stohl, A., C. Forster, A. Frank, P. Seibert, and G. Wotawa (2005), Technical note: The Lagrangian particle dispersion model FLEXPART version 6.2., *Atmos. Chem. Phys.*, *5*, 2461–2474.
Suzuki, K., T. Yamanouchi, and H. Motoyama (2008), Moisture transport to Syowa and Dome Fuji stations in Antarctica, *J. Geophys. Res.*, *113*, D24114, doi:10.1029/2008JD009794.
Thomson, D. J. (1987), Criteria for the selection of stochastic models of particle trajectories in turbulent flows, *J. Fluid Mech.*, *180*, 529–556.
Van de Berg, W. J., M. R. van den Broeke, and E. van Meijgaard (2007), Heat budget of the East Antarctic lower atmosphere derived from a regional atmospheric climate model, *J. Geophys. Res.*, *112*, D23101, doi:10.1029/2007JD008613.
van den Broeke, M. R., and N. P. M. van Lipzig (2003), Factors controlling the near-surface wind fields in Antarctica, *Mon. Weather Rev.*, *131*, 733–743.
van Lipzig, N. P. M., and M. R. van den Broeke (2002), A model study on the relation between atmospheric boundary-layer dynamics and poleward atmospheric moisture transport in Antarctica, *Tellus, Ser. A*, *54*, 497–511.
Wernli, H., and C. Schwierz (2006), Surface cyclones in the ERA-40 dataset (1958–2001). Part I: Novel identification method and global climatology, *J. Atmos. Sci.*, *63*, 2486–2507.
White, P. W. (Ed.) (2002), IFS documentation, Eur. Cent. for Medium-Range Weather Forecasts, Reading, U. K.
Wolff, E. W., and H. Cachier (1998), Concentrations and seasonal cycle of black carbon in aerosol at a coastal Antarctic station, *J. Geophys. Res.*, *103*, 11,033–11,041.
Wolff, E. W., and D. A. Peel (1985), The record of global pollution in polar snow and ice, *Nature*, *313*, 535–540.
World Meteorological Organization (1986), Atmospheric ozone 1985, *Rep. 20*, Global Ozone Res. and Monit. Proj., Geneva.
Wyputta, U. (1997), On the transport of trace elements into Antarctica using measurements at the Georg-von-Neumayer station, *Tellus, Ser. B*, *49*, 93–111.
Yurganov, L. N. (1997), Seasonal cycles of carbon monoxide over the Arctic and Antarctic: Total columns versus surface data, *Atmos. Res.*, *44*, 223–230.
Zängl, G., and K. P. Hoinka (2001), The tropopause in polar regions, *J. Clim.*, *14*, 3117–3139.

H. Sodemann and A. Stohl, Department of Regional and Global Pollution Issues, Norwegian Institute for Air Research, Instituttveien 18, N-2027 Kjeller, Norway. (ast@nilu.no)